Plasmonic Nanocages as Photothermal Transducers for Laser Induced Heating and Bubble Generation

Ioannis H. Karampelas[1], Fatema Alali[2] and Edward P. Furlani[1,2]

[1] Dept. of Chemical and Biological Engineering, [2] Dept. of Electrical Engineering,
University at Buffalo SUNY, NY 14260, Office: (716) 645-1194, Fax: (716) 645-3822, efurlani@buffalo.edu

ABSTRACT

Plasmonics is emerging from among the most promising means for generating and controlling thermal energy at the nanoscale. In this approach, metallic nanoparticles are laser heated at plasmon resonant wavelengths that depend on the size, shape and properties of the particles. Key attributes of this method include remote optical activation, nanoscale resolution and efficient photothermal transduction. In this presentation we discuss photothermal transduction using laser-pulsed colloidal gold nanocage structures. We explore fundamental aspects of this process using computational models that predict the absorption spectra of the nanoparticles, photothermal transduction at plasmon resonance, heat transfer to the fluid and the dynamics of bubble generation under conditions of superheating. We demonstrate that process variables can be tuned to achieve optimal photothermal performance. We also discuss applications involving drug delivery and therapy of malignant tumors.

Keywords: Localized surface plasmon resonance (LSPR), nanocages, plasmonic nanocages photothermal energy conversion, plasmonic-enhanced photothermal energy transfer, LSPR-induced optical absorption, pulsed-laser photothermal heating, photothermal therapy, plasmonic nanobubble cancer treatment.

1 INTRODUCTION

In recent years, there has been a proliferation of research on gold nanocages. Representing a fairly recent advance in the field of nanoparticle synthesis, such nanostructures can now be readily fabricated using bottom-up techniques [1-3]. One major advantage of this geometry is its porosity. This property makes nanocages a great nanoparticle candidate for drug encapsulation and optically controlled photothermal drug delivery [4, 5]. Moreover, nanocages have also shown increased potential for a wealth of applications including photothermal treatment [6], catalysis [7], optical imaging [8], cancer diagnosis [9] and photodynamic therapy [10] among others. Some of the most promising areas of interest involves the use of gold nanocages for cancer detection and subsequent photothermal destruction of cancer cells [11, 12]; a process where an increase in the temperature of a colloid of gold nanoparticles, preferably uptaken by cancer cells, is achieved remotely through laser irradiation, thus leading to cell apoptosis or necrosis. However, if such temperature rise is not sufficiently localized there may be unwanted damage to nearby healthy cells. Hence, the need arises to better study the diffusion and control thermal energy at the nanoscale or investigate alternative methods of treatment such as cell membrane lysis through explosive nanobubble nucleation.

Laser-based plasmonic photothermal energy conversion is of particular interest since it allows for highly localized efficient heating. In this approach, illuminating the targeted nanostructures with a pulsed laser at their plasmon resonance frequency can result in optimum energy absorption because of the coherent and collective oscillation of electrons within the nanostructures, resulting in a maximized colloidal heating effect. The plasmon resonance frequency can, in turn, be tuned from the ultraviolet (UV) through the near-infrared (NIR) spectrum by controlling their size and especially their shape during the synthesis process. [1, 2, 11-13].

Thus far, we have used computational models to elucidate the fundamental physics of plasmon-enhanced photothermal transduction for various nanoparticle geometries that exhibit some form of axial symmetry, such as nanorods, nanotori and nanorings [1, 2]. It suffices to use a 2D analysis for these structures because of their axial symmetry. In this presentation, we study the photothermal physics of laser heated plasmonic nanocages, which is more challenging since it requires a full 3D analysis. Through the use of computational models, we are able to investigate the plasmon resonance behavior of gold nanocages as a function of their geometric aspect ratios and orientation with respect to the incident polarization. We also study their thermofluidic behavior, i.e. heat transfer to the fluid and the dynamics of bubble generation under conditions of superheating. For all cases studied, we consider nanosecond-pulsed laser illumination of the nanoparticles in fluid leading to bubble nucleation, wherein the pulse duration exceeds the characteristic time constants for initial non-equilibrium photothermal transient effects. Our results show that randomly oriented nanocages are best suited for colloidal photothermal manifestation due to their higher absorption efficiency. We demonstrate that various nanocage geometries also exhibit a resonance peak in the NIR, which in combination with their high absorption in random orientations, qualify them as exceptional

photothermal transducers for deep tumor penetration and photoactivated drug delivery.

2 RESULTS AND DISCUSSION

We model laser-induced plasmon-enhanced photothermal effects using continuum-level photonic and fluidic analysis. We use computational electromagnetics to predict photothermal energy conversion within the nanoparticles, i.e. the time-averaged power absorbed by a particle as a function of the wavelength and polarization of the incident light. Subsequently, the absorbed power is converted into heat and the particle becomes a heat source within the fluid. As the particle heats up, thermal energy is transferred to the fluid and, under illumination of sufficient intensity, a vapor bubble can nucleate at the particle-fluid interface if the critical vaporization temperature of the fluid is reached. Once nucleated, a bubble will exhibit a dynamic behavior (expansion and collapse) that is a complex function of the heat and mass transfer at the bubble-fluid interface as well as the temperature and flow in the surrounding fluid. This simulation is achieved using computational fluid dynamic (CFD) analysis.

2.1 Photonic Simulations

For the photonic analysis we use 3D full-wave time-harmonic field theory. We perform the numerical simulations using the finite element-based COMSOL RF solver (wwww.comsol.com).

The first nanocage structure we consider, shown in **Fig.1,** is modeled as a hollow cubical structure with sides that are 5nm thick and 50nm in length. The nanocage is located at the origin of the computational domain and the incident field is generated by a surface current (not shown) in the xy-plane at the top of the computational domain,
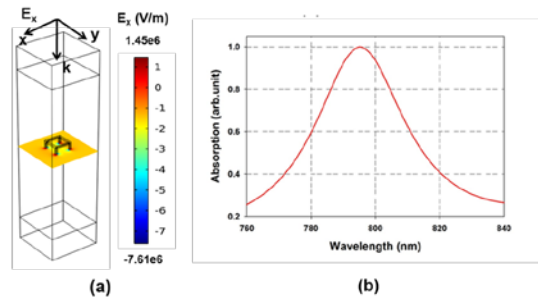

Figure 1. Photonic analysis of a gold nanocage (a= 50 nm and t = 5 nm) with parallel alignment to the incident polarization: (a) Computational domain and plot of E_x through a cross section of the domain, (b) absorbed power vs. wavelength at parallel orientation.

which results in a TEM plane wave with the electric field polarized in the x-direction and the wave propagating downwards along the z- axis as indicated by the **k** vector as shown in **Fig. 1a**. The permittivity of gold nanoparticles is predicted using an analytical expression that is based on a Drude-Lorentz model as described in our previous work [1, 2]. The parameters for this equation can be found in the literature [14-16]. We performed a parametric analysis of the power absorbed by the nanocage as a function of wavelength for λ = 760-840 nm. Plasmon resonance was found to occur at 795 nm (**Fig. 1b**).

Following our initial results, we proceeded with a parametric analysis of the absorption of a nanocage with the same dimensions at different orientations relative to the incident polarization. In **Fig. 2**, a comparison is shown between the absorption of a nanocage, of same dimensions as our initial analysis, and a nanorod with a length of 60nm and a diameter of 17nm. The absorption spectra vs. orientation of the nanocage is radically different from that of the nanorod. In the case of the nanocage, a very high
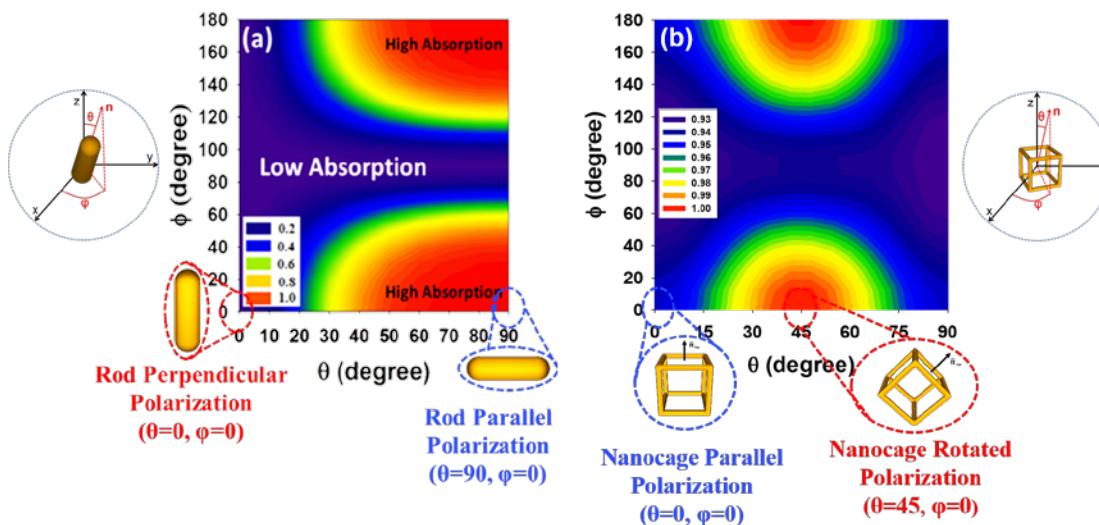
Figure 2. Normalized peak absorption at respective fixed LSPR wavelengths as a function of particle orientation (θ, φ): (a) nanorod at λ = 770 nm, (b) nanocage at λ = 795 nm [2]
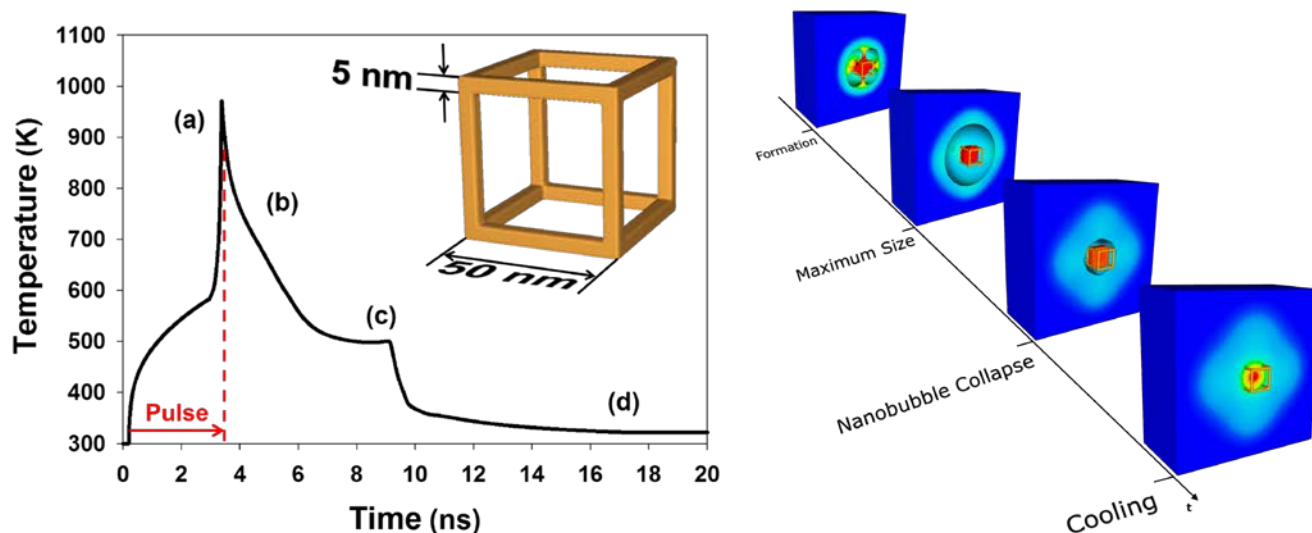
Figure 3. Photothermal heat cycle of a nanocage (a=50nm, t=5nm) (perspective 1/2 view): plot of nanocage temperature vs. time, pulse duration indicated by red arrow and dashed line and inset plots showing various phases of the thermal cycle; (a) nanobubble formation, (b) nanobubble (maximum size), (c) nanobubble collapse, (d) cooling.

absorption (more than 90%) is achieved throughout a wide range of possible orientations while in the case of the nanorod the absorption remains high only in certain favorable directions. Moreover, our results show that peak absorption for the nanocage occurs at orientations offset by 45° in an angular sense from parallel alignment with the incident field. Hence, we find that colloidal Au nanocages could be excellent as photothermal transducers for deep tumor photothermal treatment or drug delivery as they have a high transduction efficiency. This is in contrast to the nanorod where, for NIR resonance, high absorption is restricted to (near) parallel polarized orientations [2].

2.2   Fluidic Simulations

A 3D CFD analysis was implemented in order to ascertain the pulse duration and power necessary for the nucleation of an explosive nanobubble without causing potential damage to the nanostructure. Due to its symmetry, it sufficed to model one octant of the nanocage.

The fluidic analysis can be divided into two phases. In the first phase, a thermal analysis was performed to predict the power level required to heat a nanocage with an edge length of 50nm and an edge thickness of 5nm from an ambient temperature of 300K to the superheat temperature of water i.e. 580K. This depends on the pulse intensity and duration, which was constrained to be between 3 to 5 ns. In the second phase of the analysis, we applied the power levels obtained in phase one and slightly increased the pulse duration so that the nanoparticles were heated beyond the superheat temperature, which caused vaporization of the surrounding fluid and bubble nucleation. The pulse duration was tuned so that the nanoparticle achieved a temperature that was sufficiently high to generate a sustained

nanobubble, but low enough (< 1100K) to avoid melting the nanoparticle. Based on our analysis, it was found that a power of 180 μW with pulse duration of 3.18 ns is adequate for nucleation. The results of the thermo-fluidic analysis are shown in **Fig. 3**.

The nanocage and the fluid are initialized at a temperature of 300K. After 0.2 ns, a heat pulse caused by laser illumination result in a sudden rise in the temperature of the nanoparticle, which is indicated in the temperature vs. time plot of **Fig. 3**. When the nanocage reaches the superheat temperature, a homogeneous water vapor bubble is nucleated around it. Upon nucleation, the temperature of the nanoparticle rises rapidly since it is being insulated by a thin sheath of vapor while still being heated. This continues until the end of the heat pulse, which coincides with the bubble formation and maximum temperature as shown in plot segment and inset figure (a). The pulse duration is 3.18 ns as indicated by the red dashed line. After it is nucleated the nanobubble expands because of its higher pressure compared to the surrounding fluid. The nanobubble reaches a maximum size as shown in inset figure (b). For this geometry, the maximum bubble radius achieved was 120 nm. Eventually, the nanobubble collapses bringing fluid back in contact with the nanoparticle as shown in plot segment and inset figure (c), gradually reducing its temperature to the ambient temperature (d). An interesting observation of this process is the formation of a hot droplet of fluid in the middle of the nanoparticle, which partially evaporates as the nanobubble expands. The CFD simulation was performed on 12-core workstation with 64 GB of RAM. The time for the simulation was approximately 100 hours.

3 CONCLUSIONS

We have used a combination of computational electromagnetic and fluid dynamic analysis to study the effects of nanosecond-pulsed laser heating of Au nanocages. Our results demonstrate that nanocages exhibit a much higher absorption (photothermal transduction) over a wide range of orientations with respect to the incident polarization as compared to other nanoparticles with less 3D symmetry such as nanorods. Nanocages have a more than 90% average absorption for random orientations when illuminated with the appropriate plasmon resonance frequency. Hence, Au nanocage structures are well-suited as photothermal transducers and hold promise for photothermal therapy. Our modeling approach can be used to explore fundamental behavior of nanoscale photothermal processes and is useful for the rational design of novel plasmonic structures for a wide range of applications.

REFERENCES

[1] Furlani, E. P., Karampelas I. H., et al. (2012), Lab on a Chip **12**(19): 3707-3719

[2] Alali, F., Karampelas, I.H., et al. (2013), Journal of Physical Chemistry C **117**: 20178-20185

[3] Skrabalak, S.E., et al. (2008), Accounts of Chemical Research, 41(12): 1587-1595

[4] Khlebtsov, N., et al. (2013) Theranostics, 3(3): 167-180

[5] Yavuz, MS, Cheng, YY et al. (2009) Nature Materials 8(12): 935-939

[6] Chen, JY, Glaus C et al. (2010) SMALL **6**(7):811-817

[7] Zeng, J, Zhang, Q et al. (2010) Nano Letters **10**(1):30-35

[8] Cang, H, Sun, T et al. (2005) Optics Letters **30**(22):3048-3050

[9] Kim, C, Cho, EC et al. (2010) ACS Nano **4**(8):4559-4564

[10] Gao, L, Fei, JB et al. (2012) ACS Nano **6**(9):8030-8040

[11] Skrabalak, SE, Au, L et al. (2007) Nanomedicine **2**(5):657-668

[12] Chen, JY, Wang, DL et al. (2007) Nano Letters **7**(5):1328-1322

[11] West, J. L. and Halas N. J. (2000). Current Opinion in Biotechnology **11**(2): 215-217

[12] Pitsillides, C.M., et al. (2003). Biophysics Journal. **84:** 4023-4032

[13] Roper, D.K., Ahn W. et al. (2007). J. Phys. Chem. C **111**(9): 3636-3641

[14] Jain P. K., Huang X. H., et al. (2008), Acc. Chem. Res. **41**: 1578–1586

[15] Kreibig U. and Vollmer M. (1995), Optical Properties of Metal Clusters, Springer, Berlin

[16] Lewinski N., Colvin V., et al. (2008), SMALL. **4**: 26–49.